Electronic Effect on Rhodium Diphosphine Catalyzed Hydroformylation: The Bite Angle Effect Reconsidered

Lars A. van der Veen,[†] Maarten D. K. Boele,[†] Frank R. Bregman,[†] Paul C. J. Kamer,[†] Piet W. N. M. van Leeuwen,*[†] Kees Goubitz,[‡] Jan Fraanje,[‡] Henk Schenk,[‡] and Carles Bo[§]

Contribution from the Institute for Molecular Chemistry, University of Amsterdam, Nieuwe Achtergracht 166, 1018 WV Amsterdam, The Netherlands, and Department of Physical and Inorganic Chemistry, Universitat Rovira i Virgili, Plaza Imperial Tarraco 1, 43005 Tarragona, Spain

Received June 5, 1998

Abstract: The electronic effect in the rhodium diphosphine catalyzed hydroformylation was investigated. A series of electronically modified thixantphos ligands was synthesized, and their effects on coordination chemistry and catalytic performance were studied. Phosphine basicity was varied by using *p*-$(CH_3)_2N$, *p*-CH_3O, *p*-H, *p*-F, *p*-Cl, or *p*-CF_3 substituents on the diphenylphosphine moieties. X-ray crystal structure determinations of the complexes (thixantphos)Rh(CO)H(PPh_3) and (*p*-CH_3O-thixantphos)Rh(CO)H(PPh_3) were obtained. The solutions structures of the (diphosphine)Rh(CO)H(PPh_3) and (diphosphine)Rh$(CO)_2$H complexes were studied by IR and NMR spectroscopy. IR and ^{1}H NMR spectroscopy showed that the (diphosphine)Rh$(CO)_2$H complexes consist of dynamic equilibria of diequatorial (**ee**) and equatorial−apical (**ea**) isomers. The equilibrium compositions proved to be dependent on phosphine basicity; the **ee**:**ea** isomer ratio shifts gradually from almost one for the *p*-$(CH_3)_2N$-substituted ligand to more than nine for the *p*-CF_3-substituted ligand. Assignments of bands to **ee** and **ea** isomers and the shifts in wavenumbers in the IR spectra were supported by calculations on $(PH_3)_2$Rh$(CO)_2$H, $(PH_3)_2$Rh$(CO)_2$D, and $(PF_3)_2$Rh$(CO)_2$H complexes using density functional theory. In the hydroformylation of 1-octene and styrene an increase in l:b ratio and activity was observed with decreasing phosphine basicity. Most remarkably for 1-octene the selectivity for linear aldehyde formation was between 92 and 93% for all ligands. These results indicate that the chelation mode in the (diphosphine)Rh$(CO)_2$H complexes per se is not the key parameter controlling the regioselectivity. Mechanistic explanations of the effect of the natural bite angle on regioselectivity are reconsidered.

Introduction

Rhodium-catalyzed hydroformylation is one of the most important applications of homogeneous catalysis in industry.[1−5] Since the discovery of the rhodium catalysts by Wilkinson,[6,7] much effort has been made to enhance the regioselectivity of the reaction toward the formation of the more desirable linear aldehyde. High selectivities in the hydroformylation of 1-alkenes have been obtained for both diphosphite- and diphosphine-modified catalysts.[8−13] Functionalized alkenes have been hydroformylated with high selectivity by Cuny and Buchwald using rhodium diphosphite catalysts.[14] A new highly active and selective catalyst system based on binuclear rhodium complexes and tetraphosphine ligands has been developed by Stanley and co-workers.[15] Systematic studies of the correlation between phosphine structure and catalytic performance are rare, however, and despite the development of a wide variety of phosphorus ligands, no detailed understanding concerning how phosphorus ligands control selectivity has emerged.

The generally accepted dissociative mechanism for the rhodium-catalyzed hydroformylation as proposed by Wilkinson is shown in Scheme 1.[16] According to this mechanism for the hydroformylation of 1-alkenes, the selectivity is determined in the step that converts a five-coordinate L_2Rh(CO)H(alkene) into

[†] Department of Inorganic Chemistry, University of Amsterdam.
[‡] Department of Crystallography, University of Amsterdam.
[§] Universitat Rovira i Virgili.

(1) Parshall, G. W. *Homogeneous Catalysis: the applications and chemistry of catalysis by soluble transition metal complexes*; Wiley: New York, 1980.
(2) Cornils, B. In *New Syntheses with Carbon Monoxide*; Falbe, J., Ed.; Springer-Verlag: Berlin, Heidelberg, 1980; pp 1−225.
(3) Tolman, C. A.; Faller, J. W. In *Homogeneous Catalysis with Metal Phosphine Complexes*; Pignolet, L. H., Ed.; Plenum: New York, 1983; pp 81−109.
(4) Beller, M.; Cornils, B.; Frohning, C. D.; Kohlpaintner, C. W. *J. Mol. Catal. A: Chem.* **1995**, *104*, 17−85.
(5) Frohning, C. D.; Kohlpaintner, C. W. In *Applied Homogeneous Catalysis with Organometallic Compounds: a comprehensive handbook in two volumes*; Cornils, B., Herrmann, W. A., Eds.; VCH: Weinheim, New York, Basel, Cambridge, Tokyo, 1996; Vol. 1, pp 27−104.
(6) Evans, D.; Yagupsky, G.; Wilkinson, G. *J. Chem. Soc. A* **1968**, 2660−2665.
(7) Brown, C. K.; Wilkinson, G. *J. Chem. Soc. A* **1970**, 2753−2764.
(8) Buisman, G. J. H.; Vos, E. J.; Kamer, P. C. J.; van Leeuwen, P. W. N. M. *Tetrahedron: Asymmetry* **1995**, *6*, 719−738.
(9) van Rooy, A.; Kamer, P. C. J.; van Leeuwen, P. W. N. M.; Goubitz, K.; Fraanje, J.; Veldman, N.; Spek, A. L. *Organometallics* **1996**, *15*, 835−847.
(10) Kranenburg, M.; van der Burgt, Y. E. M.; Kamer, P. C. J.; van Leeuwen, P. W. N. M. *Organometallics* **1995**, *14*, 3081−3089.
(11) Billig, E.; Abatjoglou, A. G.; Bryant, D. R. (to Union Carbide Corp.) U.S. Patent 4.769.498, 1988.
(12) Devon, T. J.; Phillips, G. W.; Puckette, T. A.; Stavinoha, J. L.; Vanderbilt, J. J. (to Eastman Kodak) U.S. Patent 4,694,109, 1987.
(13) Burke, P. M.; Garner, J. M.; Tam, W.; Kreutzer, K. A.; Teunissen, A. J. J. M.; Snijder, C. S.; Hansen, C. B. (to DSM/Du Pont de Nemours) WO 97/33854, 1997.
(14) Cuny, G. D.; Buchwald, S. L. *J. Am. Chem. Soc.* **1993**, *115*, 2066−2068.
(15) Broussard, M. E.; Juma, B.; Train, S. G.; Peng, W.-J.; Laneman, S. A.; Stanley, G. G. *Science* **1993**, *260*, 1784−1788.
(16) Evans, D.; Osborn, J. A.; Wilkinson, G. *J. Chem. Soc. A* **1968**, 3133−3142.

10.1021/ja981969e CCC: $15.00
Published on Web 11/03/1998

Scheme 1

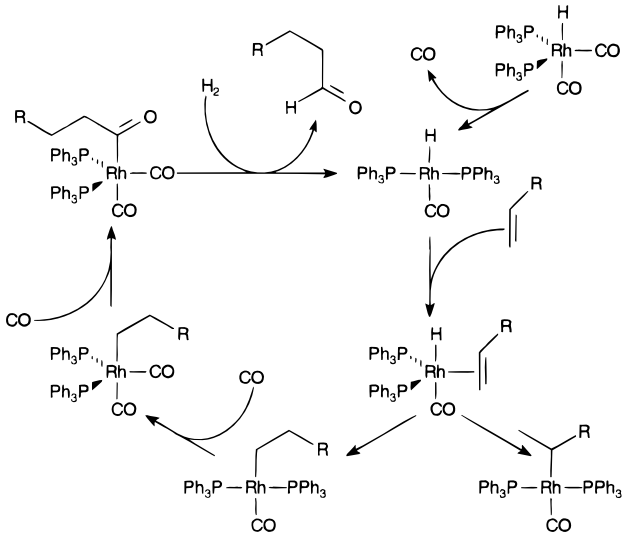

either a linear or branched four-coordinate $L_2Rh(CO)(alkyl)$. For the linear rhodium alkyl species this step is irreversible at moderate temperatures and sufficiently high pressures of CO. The structure of the alkene complex is therefore thought to play a crucial role in controlling the regioselectivity.[17,18] However, contrary to the $L_2Rh(CO)_2H$ precursor complex, the $L_2Rh(CO)H$(alkene) intermediate has not been observed directly so far. Brown and Kent have shown that the PPh_3-modified precursor complex $(PPh_3)_2Rh(CO)_2H$ exists as a mixture of two rapidly equilibrating trigonal bipyramidal isomers in a diequatorial (**ee**) to equatorial−apical (**ea**) isomer ratio of 85:15.[19,20]

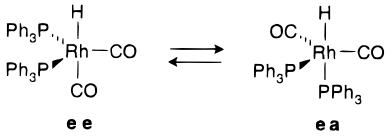

The stereoelectronic properties of phosphorus ligands have a dramatic influence on the reactivity of hydroformylation catalysts. Tolman introduced the concept of cone angle θ and the electronic parameter χ as measures of respectively the steric bulk and the electronic properties of phosphorus ligands.[21,22] Casey and co-workers developed the concept of the natural bite angle as an additional characteristic of diphosphine ligands based on molecular mechanics calculations.[23] The pronounced effect of the natural bite angle on the selectivity in the hydroformylation was shown by Casey and co-workers as well as by our group.[10,17]

While a rational understanding of how ligand structure can steer the selectivity in the hydroformylation is now unfolding, only limited attention has been paid to the electronic properties of phosphine ligands and their influence on catalytic performance.[24] In one of the few detailed studies, Moser and co-workers investigated the effect of phosphine basicity in the hydroformylation by using a series of *p*-substituted triphenylphosphines.[25] Diphosphines of different basicities were studied by Unruh and Christenson.[26] Both studies showed that less basic phosphines afford higher reaction rates and higher linear over branched (l:b) ratios. In a recent study Casey and co-workers investigated the electronic effect of equatorial and apical phosphines.[27] They concluded that electron-withdrawing substituents on phosphines in the equatorial position give high l:b ratios, while electron-withdrawing substituents on phosphines in the apical position give low l:b ratios. The results of this study, however, cannot be described in terms of electronic effects only, since there are major steric differences between the **ee** and **ea** coordinating diphosphines.

Table 1. Selected Data for Ligands **1**−**7**

ligand	R	β_n,[a] deg	flexibility range,[a] deg	χ_i,[b] cm^{-1}	σ_p[c]
1	$N(CH_3)_2$	109.1	92−124	1.8	−0.83
2	OCH_3	106.9	91−123	3.4	−0.27
3	CH_3	106.7	91−125	3.5	−0.17
4	H	106.4	91−127	4.3	0.00
5	F	106.6	92−128	5.0	0.06
6	Cl	107.8	91−126	5.6	0.23
7	CF_3	109.3	92−128	6.6	0.54

[a] The natural bite angle (β_n) and the flexibility range were calculated analogously to the method used by Casey and Whiteker.[23] β_n is defined as the preferred chelation angle determined only by ligand backbone constraints and not by metal valence angles. The flexibility range is defined as the accessible range of bite angles within less than 3 kcal mol^{-1} excess strain energy from the calculated natural bite angle. [b] Tolman χ_i values were abstracted from ref 28. [c] Hammett σ_p values were abstracted from ref 29.

To study the exact nature of the electronic effect in the rhodium diphosphine catalyzed hydroformylation, we synthesized a series of thixantphos[10] ligands with varying basicity (**1**−**7**,

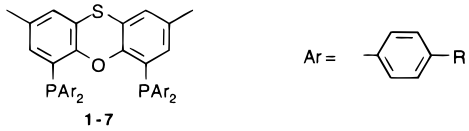

Table 1) and probed their catalytic performance and coordination chemistry in rhodium complexes. In this series of ligands, steric differences are minimal so purely electronic effects can be investigated. Here we report that the equilibrium between **ee** and **ea** coordination in the $(diphosphine)Rh(CO)_2H$ complexes is dependent on phosphine basicity. Decreasing phosphine basicity shifts the equilibrium to **ee** coordination. In the hydroformylation of 1-octene and styrene decreasing phosphine basicity gives an increase both in l:b ratio and in activity, while increasing phosphine basicity gives the opposite effect. Most remarkably, for 1-octene, selectivity for linear aldehyde remains virtually the same, 92−93%, due to the enhanced isomerization activity displayed by the less basic phosphines. These results show that the electronic properties of the diphosphine ligands and their coordination mode in the $(diphosphine)Rh(CO)_2H$ complexes do not influence the regioselectivity. Mechanistic implications and possible explanations for the bite angle effect are discussed.

(17) Casey, C. P.; Whiteker, G. T.; Melville, M. G.; Petrovich, L. M.; Gavney, J. A., Jr.; Powell, D. R. *J. Am. Chem. Soc.* **1992**, *114*, 5535−5543.
(18) Casey, C. P.; Petrovich, L. M. *J. Am. Chem. Soc.* **1995**, *117*, 6007−6014.
(19) Brown, J. M.; Kent, A. G. *J. Chem. Soc., Perkin Trans. 2* **1987**, 1597−1607.
(20) Throughout this work, notations **ee** and **ea** refer to respectively the diequatorial and equatorial−apical chelation modes of the diphosphine in trigonal bipyramidal rhodium complexes.
(21) Tolman, C. A. *Chem. Rev.* **1977**, *77*, 313−348.
(22) Tolman, C. A. *J. Am. Chem. Soc.* **1970**, *92*, 2953−2956.
(23) Casey, C. P.; Whiteker, G. T. *Isr. J. Chem.* **1990**, *30*, 299−304.
(24) Oswald, A. A.; Hendriksen, D. E.; Kastrup, R. V.; Mozeleski, E. J. *Adv. Chem. Ser.* **1992**, *230*, 395−418.
(25) Moser, W. R.; Papile, C. J.; Brannon, D. A.; Duwell, R. A.; Weininger, S. J. *J. Mol. Catal.* **1987**, *41*, 271−292.
(26) Unruh, J. D.; Christenson, J. R. *J. Mol. Catal.* **1982**, *14*, 19−34.
(27) Casey, C. P.; Paulsen, E. L.; Beuttenmueller, E. W.; Proft, B. R.; Petrovich, L. M.; Matter, B. A.; Powell, D. R. *J. Am. Chem. Soc.* **1997**, *119*, 11817−11825.

Scheme 2[a]

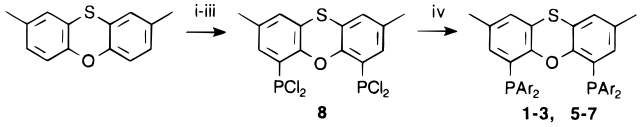

[a] (i) *n*-BuLi/TMEDA/Et_2O/25 °C; (ii) $ZnCl_2$/0 °C; (iii) PCl_3/−110 °C; (iv) ArMgBr/THF/0 °C.

Results

Synthesis of Thixantphos Ligands Containing Electron-Donating and Electron-Withdrawing *p*-Substituents. The thixantphos ligands were synthesized by reacting the Grignard reagent of the appropriate *p*-substituted aryl bromide with 4,5-bis(dichlorophosphino)-2,7-dimethylphenoxathiin (**8**) (Scheme 2). Compound **8** was prepared by selective dilithiation of 2,7-dimethylphenoxathiin followed by reaction with zinc chloride and reaction of the resulting dizinc compound with an excess of phosphorus trichloride at low temperature.[30] Typical yields of the ligands varied from 25% for *p*-CH_3O-thixantphos (**2**) to 54% for *p*-$(CH_3)_2N$-thixantphos (**1**) based on **8.** Table 1 shows that variation of the substituent has only a minor effect on the natural bite angle and flexibility range and, therefore, steric effects can be neglected when evaluating the electronic influence of these ligands in catalysis.[31]

Rhodium Complexes. To investigate the influence of phosphine basicity on chelation behavior, the solution structures of the (diphosphine)Rh(CO)H(PPh_3) complexes and the (diphosphine)Rh(H)$(CO)_2$ complexes were studied in great detail for all ligands. Displacement of PPh_3 in $(PPh_3)_3$Rh(CO)H by the diphosphines **1**−**7** resulted in formation of the (diphosphine)-Rh(CO)H(PPh_3) complexes **9a**−**15a**. Crystals of the (diphosphine)Rh(CO)H(PPh_3) complexes suitable for X-ray structure determination were obtained for ligands **2** and **4**.

The X-ray crystal structures of (*p*-CH_3O-thixantphos)Rh-(CO)H(PPh_3) (**10a**) and (Thixantphos)Rh(CO)H(PPh_3) (**12a**) are very similar so only the latter is shown in Figure 1. Selected bond lengths and angles of both complexes are given in Table 2. The crystal structures reveal distorted trigonal bipyramidal complex geometries with all phosphines occupying equatorial sites. In the structures the Rh atom is located slightly above the equatorial plane defined by the three phosphorus atoms and displaced toward the apical carbonyl ligand. The hydride ligand was located in neither structures, but ^{1}H NMR indicates that it occupies the apical site trans to the carbonyl ligand (vide infra). The P−Rh−P bite angles are 111.73(5)° for the thixantphos ligand and 109.31(7)° for the *p*-CH_3O-thixantphos ligand. The small difference in observed bite angles between *p*-CH_3O-thixantphos and the unsubstituted thixantphos confirms our assumption based on molecular mechanics that *p*-substitution on the aryl rings has only minor steric effects. A noticeable difference between comparable bond lengths in the complexes is found in the Rh−CO distance. The decreased Rh−CO bond length for the *p*-CH_3O-thixantphos complex (1.863(8) Å) compared to the thixantphos complex (1.887(8) Å) is a direct result of increased back-bonding of the rhodium to the carbonyl ligand (vide infra).

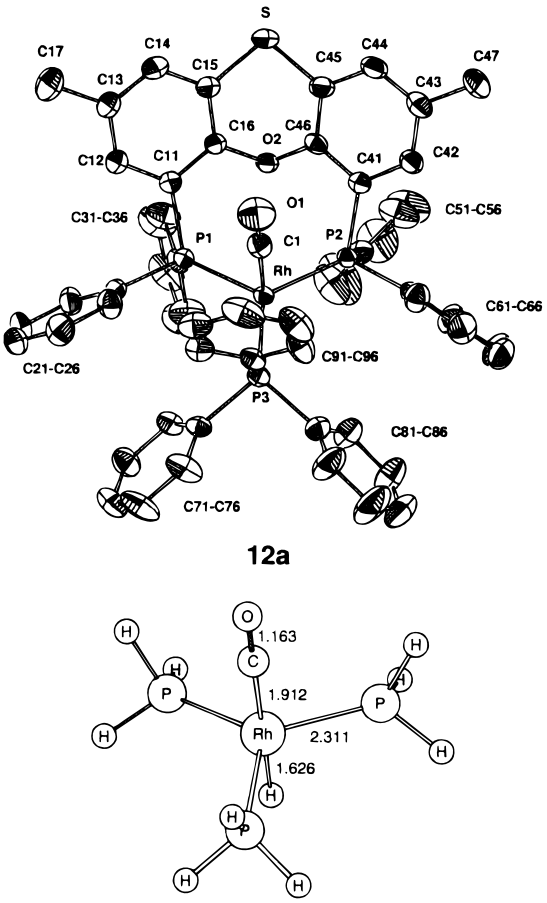

Figure 1. X-ray structure and numbering scheme for (thixantphos)-Rh(CO)H(PPh_3) (**12a**) (hydrogen atoms have been omitted for clarity) and optimized geometry of $(PH_3)_3$Rh(CO)H (bond lengths are given in angstroms).

Table 2. Selected Bond Lengths and Angles for (Thixantphos)Rh(CO)H(PPh_3) (**12a**) and (*p*-CH_3O-Thixantphos)Rh(CO)H(PPh_3) (**10a**)

(thixantphos)Rh(CO)H(PPh_3) (**12a**)		(*p*-CH_3O-thixantphos)Rh(CO)H(PPh_3) (**10a**)	
	Bond Lengths (Å)		
Rh−P(1)	2.327(1)	Rh−P(1)	2.313(2)
Rh−P(2)	2.318(1)	Rh−P(2)	2.328(2)
Rh−P(3)	2.295(2)	Rh−P(3)	2.292(2)
Rh−C(1)O	1.887(8)	Rh−C(61)O	1.863(8)
	Bond Angles (deg)		
P(1)−Rh−P(2)	111.73(5)	P(1)−Rh−P(2)	109.31(7)
P(1)−Rh−P(3)	121.73(5)	P(1)−Rh−P(3)	126.65(8)
P(2)−Rh−P(3)	124.53(5)	P(2)−Rh−P(3)	121.65(7)
P(1)−Rh−C(1)	94.2(2)	P(1)−Rh−C(61)	94.4(2)
P(2)−Rh−C(1)	94.9(2)	P(2)−Rh−C(61)	96.9(3)
P(3)−Rh−C(1)	95.0(2)	P(3)−Rh−C(61)	94.2(3)

Calculated Structure for the $(PH_3)_3$Rh(CO)H Complex. To support the spectroscopic results of the (diphosphine)Rh-(CO)H(PPh_3) complexes (vide infra), calculations were performed on the $(PH_3)_3$Rh(CO)H complex using density functional theory (DFT). The geometry of the $(PH_3)_3$Rh(CO)H complex was optimized under the constraints of the C_{3v} symmetry group and characterized as a minimum from the vibrational analysis. The structure is depicted in Figure 1. The calculated Rh−P and Rh−C bond lengths and the H−Rh−C angle are in good agreement with the distorted trigonal bipyramidal symmetry observed in the X-ray structures of complexes **10a** and **12a**. Recently Schmid and co-workers also reported on the optimized

(28) Dias, P. B.; de Piedade, M.; Simoes, J. A. M. *Coord. Chem. Rev.* **1994**, *135/136*, 737−807.
(29) Hansch, C.; Leo, A.; Taft, R. W. *Chem. Rev.* **1991**, *91*, 165−195.
(30) Private communication of Dr. H. T. Teunissen and Prof. Dr. F. Bickelhaupt.
(31) It should be noted that in the MM2 calculations the same approximate parameters are used for phosphorus and rhodium, despite electronic changes.

Table 3. Selected IR Data for (Diphosphine)Rh(CO)H(PPh_3) Complexes **9a**−**15a**[a]

ligand	R	ν_1, cm^{-1}	ν_2, cm^{-1}
9a	$N(CH_3)_2$	1982 (s)	1909 (m)
10a	OCH_3	1989 (s)	1916 (m)
11a	CH_3	1999 (s)	1920 (m)
12a	H	1999 (s)	1922 (w)
13a	F	2001 (s)	1921 (m)
14a	Cl	2006 (s)	1928 (m)
15a	CF_3	2009 (s)	1931 (m)

[a] In KBr, carbonyl region.

structure of the $(PH_3)_3Rh(CO)H$ complex obtained by DFT calculations.[32] The geometry parameters they obtained at the LDA level of theory are very similar to the values presented here.

NMR Data for (Diphosphine)Rh(CO)H(PPh_3) Complexes 9a−15a. The presence of hydride ligands in all (diphosphine)-Rh(CO)H(PPh_3) complexes is confirmed by ^{1}H NMR. The rhodium hydride signals appear as broadened quartets or triplets of doublets at $\delta = -9.09$ to -9.60 (td, ^2J(P,H) = 10−21 Hz). The rhodium-proton coupling constants could not be resolved. The phosphorus−proton coupling constants are consistent with hydrides occupying apical positions cis to three equatorial phosphines in distorted trigonal bipyramidal complex geometries (vide supra). Evaluation of the ^{31}P{^{1}H} NMR spectra leads to the conclusion that for all complexes the two phosphine moieties of the diphosphine in the complex are equivalent. The diphosphine P−PPh_3 coupling constants (^2J(P,P) = 123−126 Hz) are also in agreement with structures in which all phosphines occupy equatorial sites.

IR Data for (Diphosphine)Rh(CO)H(PPh_3) Complexes 9a−15a. The IR frequencies of the (diphosphine)Rh(CO)-H(PPh_3) complexes in the carbonyl region display a clear electronic effect (Table 3). The IR spectra of the complexes in KBr all have two absorption bands between 1900 and 2100 cm^{-1} due to combination bands of ν_{RhH} and ν_{CO}. Both bands show a regular shift to higher wavenumbers with decreasing phosphine basicity. The lower electron density on the metal leads to a decrease in back-bonding from the rhodium to the carbonyl ligand, and hence, higher CO stretching frequencies are observed. The experimental results are in good correlation with the results of the DFT calculations on the $(PH_3)_3Rh(CO)H$ complex. The calculated IR spectrum also exhibits two harmonic frequencies: one at 1911 cm^{-1} corresponding to the symmetric combination of the Rh−H and the Rh−CO vibrations and one at 2007 cm^{-1} corresponding to the antisymmetric combination of the same vibrations.

Calculated Structures for $(PH_3)_2Rh(CO)_2H$ and $(PF_3)_2Rh(CO)_2H$ Complexes. To model the basicity-dependent features exhibited by the (diphosphine)$Rh(CO)_2H$ complexes (vide infra), DFT calculations were performed on the $(PH_3)_2Rh(CO)_2H$ and $(PF_3)_2Rh(CO)_2H$ complexes. Similar calculations of the equilibrium structures of four- and five-coordinate rhodium hydrido carbonyl complexes using PH_3 as model ligand have been reported recently by Schmid and co-workers.[32] The **ee** and **ea** isomers of both complexes were fully optimized imposing C_s symmetry (Figure 2). Bond lengths and angles are listed in Table 4. A clear dependence on phosphine basicity is observed for almost all parameters. Upon changing the basic PH_3 ligand for the less basic PF_3 ligand, C−O distances decrease while Rh−C distances increase as a direct result of the reduced back-bonding to the carbonyl ligands. A large

(32) Schmid, R.; Herrmann, W. A.; Frenking, G. *Organometallics* **1997**, *16*, 701−708.

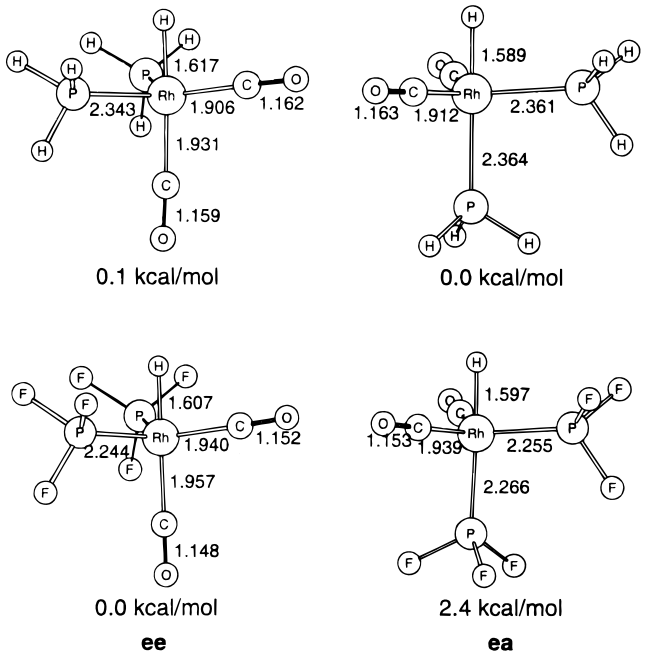

Figure 2. Optimized geometries of the $(PH_3)_2Rh(CO)_2H$ and $(PF_3)_2$-$Rh(CO)_2H$ complexes together with the relative energy of the **ee** and **ea** isomers. Bond lengths are given in angstroms.

Table 4. Calculated Structural Data for **ee** and **ea** Isomers of Complexes $(PH_3)_2Rh(CO)_2H$ and $(PF_3)_2Rh(CO)_2H$[a]

	$(PH_3)_2Rh(CO)_2H$		$(PF_3)_2Rh(CO)_2H$	
	ee	**ea**	**ee**	**ea**
Rh−H (Å)	1.617	1.589	1.607	1.597
Rh−$P_{e/a}$ (Å)	2.343	2.361/2.364	2.244	2.255/2.266
Rh−$C_{e/a}$ (Å)	1.906/1.931	1.912	1.940/1.957	1.939
C−$O_{e/a}$ (Å)	1.162/1.159	1.163	1.152/1.148	1.153
H−Rh−$P_{e/a}$ (deg)	84.2	85.5/179.7	82.4	84.9/177.5
H−Rh−$CO_{e/a}$ (deg)	82.7/177.4	84.6	82.2/179.5	82.3
P−Rh−P (deg)	110.1	94.8	112.5	97.6

[a] The subscripts e and a denominate equatorial and apical ligand positions.

decrease in Rh−P bond lengths (0.1 Å) is observed with decreasing phosphine basicity, accompanied by a slight increase in P−Rh−P angle. The increase in P−Rh−P angle is, however, most likely not an electronic but a steric effect. Unlike the other parameters the effect of phosphine basicity on the Rh−H bond length differs for each isomer; for the **ee** isomer the Rh−H distance decreases with decreasing phosphine basicity, while for the **ea** isomer the opposite occurs. Comparison of the P−Rh−P angles of the calculated complexes with the flexibility ranges in Table 1 shows that both **ee** and **ea** isomers of the (diphosphine)$Rh(CO)_2H$ complexes could be accessible for the thixantphos ligands.

HP NMR Data for (Diphosphine)Rh$(CO)_2$H Complexes 9b−15b. For all diphosphine ligands, the formation of the (diphosphine)$Rh(CO)_2H$ complexes was evidenced by the appearance of a doublet in the ^{31}P NMR spectra and an apparent triplet of doublets for the rhodium hydride in the ^{1}H NMR spectra. Table 5 reveals that decreasing phosphine basicity gives decreasing rhodium−proton (^1J(Rh,H)) and phosphorus−proton (^2J(P,H)) coupling constants but increasing rhodium−phosphorus (^1J(Rh,P)) coupling constants.[33]

(33) ^{103}Rh NMR data will be reported elsewhere.

Table 5. Selected NMR Data for (Diphosphine)Rh(CO)$_2$H Complexes **9b**−**15b**[a]

ligand	R	^1J(Rh,H), Hz	^1J(Rh,P), Hz	$^2J_{av}$(P,H), Hz	% **ee**[b]
9b	$N(CH_3)_2$	8.7	121	27.9	44−50
10b	OCH_3	7.5	124	21.6	56−62
11b	CH_3	7.2	126	17.6	63−69
12b	H	6.6	128	14.7	69−75
13b	F	6.3	130	11.0	76−83
14b	Cl	6.0	132	8.4	81−88
15b	CF_3	4.5	134	3.6	89−96

[a] In C_6D_6 at 298 K. [b] Calculated from the $^2J_{av}$(P,H) using trans ^2J(P,H) = 106 Hz and cis ^2J(P,H) ≤ ±2 Hz.

The rhodium−proton and phosphorus−proton coupling constants and their dependence on phosphine basicity suggest that these complexes exist as mixtures of **ee** and **ea** isomers that are in dynamic equilibrium.[19] Rapid interconversion of the two isomers, presumably via pseudo-Berry rotations, interchanges the phosphorus atoms, and therefore, averaged chemical shifts and coupling constants are observed. As demonstrated by Yagupsky and Wilkinson and recently by Casey and co-workers for related iridium complexes,[27,34] the ratio of the two isomers can be calculated from the averaged observed coupling constant if all separate values are known. Unfortunately the dynamic equilibria of the complexes could not be frozen out even at 163 K, so the coupling constants for the individual isomers could not be determined. Estimations of the complex mixture compositions at room temperature were achieved using a cis phosphorus−proton coupling of −2 to 2 Hz, and a trans phosphorus−proton coupling of 106 Hz.[35] From the calculated complex mixture compositions it can be concluded that the equilibrium between the **ee** and **ea** isomer is greatly influenced by phosphine basicity. For the strongly electron-donating $N(CH_3)_2$ substituent, the **ea** isomer is slightly favored, while for the strongly electron-withdrawing CF_3 substituent, the equilibrium is shifted almost completely to the **ee** isomer.

The enhanced preference of the basic phosphines for apical coordination and the preference of the nonbasic phosphines for equatorial coordination is quantitatively demonstrated by our DFT calculations on the **ee** and **ea** isomers of complexes $(PH_3)_2$-Rh(CO)$_2$H and $(PF_3)_2$Rh(CO)$_2$H (Figure 2). The energy difference between the **ee** and **ea** isomer of the complex modified with PH_3 as model ligand for a basic phosphine was calculated to be 0.1 kcal mol^{-1} in favor of the **ea** isomer. This small energy difference would correspond to an **ee**:**ea** equilibrium composition of approximately 1:1 at room temperature.[36] A slight preference of the **ea** isomer over the **ee** isomer for the PH_3 ligand has also been reported by Schmid and co-workers and by Matsubara and co-workers.[32,37] With PF_3 as a model ligand for a nonbasic phosphine the **ee** isomer was found to be favored by 2.4 kcal mol^{-1}. This corresponds to an **ee**:**ea** equilibrium ratio of approximately 50:1 at room temperature. The calculated shift of the equilibrium upon changing the basic PH_3 ligand for the less basic PF_3 ligand is consistent with the observed shift in isomer composition with decreasing phosphine basicity in the series of substituted thixantphos ligands.

HP-IR Data for (Diphosphine)Rh(CO)$_2$H Complexes 9b−15b. Unambiguous evidence for the existence of a dynamic equilibrium between **ee** and **ea** complex isomers was supplied by HP-IR spectroscopy. The spectra of the (diphosphine)Rh-(CO)$_2$H complexes all showed four absorption bands in the carbonyl region (Figure 3).

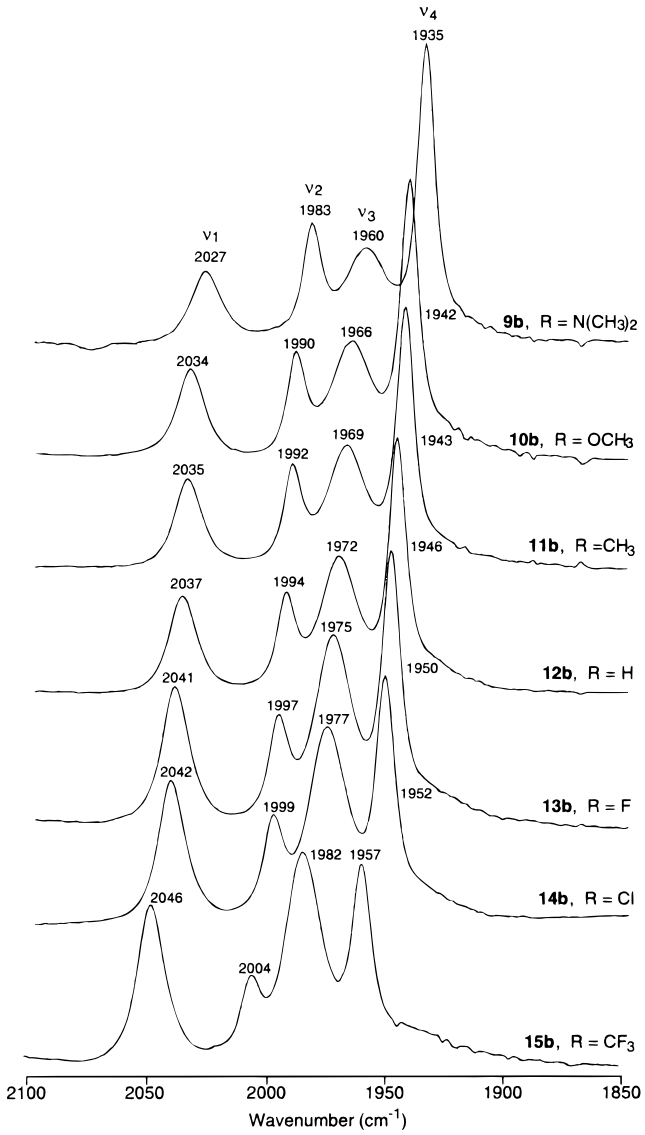

Figure 3. HP-IR spectra for (diphosphine)Rh(CO)$_2$H complexes **9b**−**15b** in 2-Me-THF at 80 °C and 20 bar of CO/H$_2$ (1:1) (carbonyl region).

In an effort to assign the bands to **ee** and **ea** isomers the (thixantphos)Rh(CO)$_2$D complex was measured for comparison. Upon H/D exchange, only ν_1 and ν_3 shift to lower wavenumbers (respectively 18 and 14 cm^{-1}), and therefore, these two bands are assigned to the carbonyls of the **ee** complex.[38] The two remaining bands that do not shift, ν_2 and ν_4, belong consequently to the **ea** complex. From the disappearance of a low-frequency shoulder upon H/D exchange, it can be concluded that one of the rhodium hydride vibrations is partly hidden under ν_4.

To verify the empirical peak assignments, the theoretical IR spectra of the $(PH_3)_2$Rh(CO)$_2$H and -D and $(PF_3)_2$Rh(CO)$_2$H complexes were calculated by DFT methods. Recently several reports have been published concerning the calculation of

(34) Yagupsky, G.; Wilkinson, G. *J. Chem. Soc. A* **1969**, 725−733.

(35) A trans phosphorus−proton coupling of 106 Hz was observed in ^{1}H NMR spectrum of the **ea** isomer of (DPEphos)Rh(CO)$_2$H at 173 K (unpublished results).

(36) By the calculation of the complex mixture composition entropy terms are neglected.

(37) Matsubara, T.; Koga, N.; Ding, Y.; Musaev, D. G.; Morokuma, K. *Organometallics* **1997**, *16*, 1065−1078.

(38) H/D exchange will only effect the **ee** isomer because in this isomer there is a trans relationship between the hydride and a carbonyl ligand which results in coupling of the vibrations. The disappearance of resonance interaction upon H/D exchange will lead to frequency shifts of the carbonyl bands of the **ee** isomer.

Table 6. Calculated Rh−H, Rh−D, and C−O Stretching Harmonic Frequencies, IR Intensities, and Assignments for the **ee** and **ea** Isomers of Complexes $(PH_3)_2Rh(CO)_2D$, $(PH_3)_2Rh(CO)_2H$, and $(PF_3)_2Rh(CO)_2H$[a]

$(PH_3)_2Rh(CO)_2D$			$(PH_3)_2Rh(CO)_2H$			$(PF_3)_2Rh(CO)_2H$	
frequency, cm^{-1}	intensity, km/mol	assignment	frequency,[b] cm^{-1}	intensity, km/mol	assignment	frequency, cm^{-1}	intensity, km/mol
ee isomer							
2006	638	$(C-O)_e+(C-O)_a$	2041 (2087)	532	$(Rh-H)-(C-O)_e-(C-O)_a$	2099	423
1963	924	$(C-O)_e-(C-O)_a$	1983 (2043)	705	$(Rh-H)+(C-O)_e+(C-O)_a$	2036	555
1414	14	Rh-D	1938 (1961)	371	$(Rh-H)-(C-O)_e+(C-O)_a$	2004	279
ea isomer							
			2069 (2049)	138	Rh−H	2062	52
1985	477	(C−O)+(C−O)	1985 (2061)	478	(C−O)+(C−O)	2042	374
1948	1223	(C−O)−(C−O)	1948 (2028)	1224	(C−O)−(C−O)	2010	1035
1470	61	Rh−D					

[a] Assignments based on the normal modes analysis, the subscripts e and a denominate equatorial and apical ligand positions, and the signs indicate equal (+) or different (−) phase between the vibration of each bond. [b] The values in parentheses were reported by Schmid and coworkers.[32]

harmonic frequencies of carbonyl ligands in metal−carbonyl complexes and we have used the same methodology as described in some of them.[39−41] The calculated harmonic vibrational frequencies, intensities, and the corresponding assignments based on the normal modes analysis of the carbonyl vibrations are depicted in Table 6. Comparison of the frequencies of $(PH_3)_2Rh(CO)_2H$ and -D shows that H/D exchange only effects the carbonyl frequencies of the **ee** isomer of the complex. The calculated shift to lower frequency of the vibrations of the **ee** isomer is in perfect agreement with the observed spectra and confirms the empirical peak assignment to **ee** and **ea** isomers. The fit of the absolute values of the calculated frequencies of $(PH_3)_2Rh(CO)_2H$ with the measured values of the series (thixantphos)$Rh(CO)_2H$ complexes (Figure 3) is striking. Only the calculated value for ν_3 (1983 cm^{-1}) is out of the range of ν_3 values obtained experimentally (1960−1982 cm^{-1}).

The effect of decreasing phosphine basicity on the theoretical IR spectra is an overall increase in frequency and a decrease in intensity of the vibrations. The only vibration that does not experience a positive shift of approximately 60 cm^{-1} upon exchanging PH_3 for PF_3, is the Rh−H frequency of the **ea** isomer. Instead the decreased Rh−H bond length (vide supra) results in a shift of 7 cm^{-1} to lower frequency. The low calculated intensities for the Rh−H vibrations of the **ea** isomers explain the absence of the corresponding Rh−H bands in the spectra of the different (thixantphos)$Rh(CO)_2H$ complexes (Figure 3). The calculated frequencies and intensities of the **ee** isomers are in good agreement with the assignment of low-frequency shoulders of ν_4 to Rh−H signals in the observed spectra (Figure 3).

The shift in isomer composition that was found in the NMR spectra is confirmed and clearly visualized when comparing the IR spectra of the series of complexes (Figure 3). Going from electron-donating substituents to electron-withdrawing substituents, the intensities of the absorption bands of the **ea** isomer are diminished in favor of those of the **ee** isomer. Another trend observed in the series is a regular shift to higher wavenumbers of all four absorption bands with decreasing phosphine basicity. These shifts are comparable to the ones found for the (diphosphine)$Rh(CO)H(PPh_3)$ complexes.

The IR spectra of the rhodium species present during actual hydroformylation experiments with ligands **2**, **4**, and **7** and the respective (diphosphine)$Rh(CO)_2H$ complexes are identical. The **ee**:**ea** equilibria are not influenced, and no other carbonyl complexes are observed. The observation that the (diphosphine)$Rh(CO)_2H$ complexes are the only rhodium carbonyl species present during hydroformylation implies that the rate-determining step is located early in the catalytic cycle. Either CO dissociation or, more likely, alkene coordination will be rate determining (Scheme 1).[26] Evidence for rate-limiting alkene coordination can be found in increasing reaction rates with decreasing CO pressure, increasing alkene concentration, and decreasing phosphine basicity (vide infra).

Table 7. Results of the Hydroformylation of 1-Octene at 80 °C[a]

ligand	R	σ_p	l:b ratio[b]	% select[b]	% isomer[b]	tof[b,c]
1	$N(CH_3)_2$	−0.83	44.6	93.1	4.8	28
2	OCH_3	−0.27	36.9	92.1	5.3	45
3	CH_3	−0.17	44.4	93.2	4.7	78
4	H	0.00	50.0	93.2	4.9	110
5	F	0.06	51.5	92.5	5.7	75
6	Cl	0.23	67.5	91.7	6.9	66
7	CF_3	0.54	86.5	92.1	6.8	158

[a] Conditions: $CO/H_2 = 1$, $P(CO/H_2) = 20$ bar, ligand/Rh = 5, substrate/Rh = 637, [Rh] = 1.00 mM, number of experiments = 3. In none of the experiments was hydrogenation observed. [b] Linear over branched ratio, percent selectivity for linear aldehyde, percent isomerization to 2-octene, and turnover frequency were determined at 20% alkene conversion. [c] Turnover frequency = (mol of aldehyde) (mol of Rh)$^{-1}$ h^{-1}.

Hydroformylation of 1-Octene. Hydroformylation of 1-octene was carried out at 80 °C and 20 bar of 1:1 CO/H_2 using a 1.0 mM solution of rhodium diphosphine catalyst prepared from $Rh(CO)_2$(dipivaloylmethanoate) (dpm) and 5 equiv of ligand. The production of octene isomers, nonanal, and 2-methyloctanal was monitored by gas chromatography. The results of the experiments with ligands **1**−**7** are shown in Table 7. Turnover frequencies were determined at 20% conversion.

Table 7 shows that, with the exception of ligands **5** and **6**, the rate of the reaction increases with decreasing phosphine basicity. An explanation for the deviant behavior of **5** and **6** can be incomplete catalyst formation or deactivation of the catalyst.

The inverse dependency of the reaction rate on the phosphine basicity is often found in the rhodium-catalyzed hydroformylation.[25,26] Decreasing phosphine basicity facilitates CO dissociation from the (diphosphine)$Rh(CO)_2H$ complex and enhances alkene coordination to form the (diphosphine)Rh(CO)H(alkene) complex, and therefore, the reaction rate increases. Weakening of the rhodium−carbonyl bond in the rhodium carbonyl complexes by electron-withdrawing substituents on the

(39) Ehlers, A. W.; Frenking, G.; Baerends, E. J. *Organometallics* **1997**, *16*, 4896−4902.
(40) Ehlers, A. W.; Ruiz-Morales, Y.; Baerends, E. J.; Ziegler, T. *Inorg. Chem.* **1997**, *36*, 5031−5036.
(41) Barckholtz, T. A.; Bursten, B. E. *J. Am. Chem. Soc.* **1998**, *120*, 1926−1927.

Scheme 3

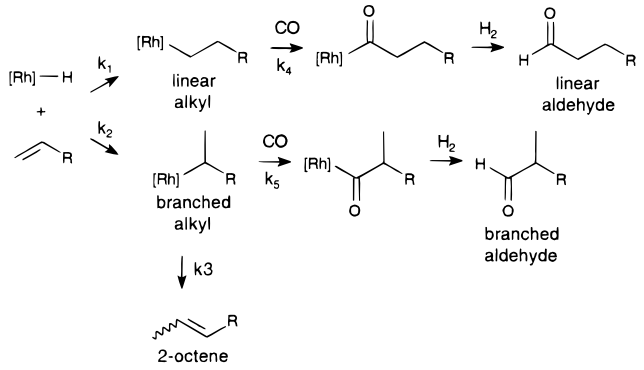

ligand is evidenced by an increase in carbonyl stretching frequencies (vide supra).

Surprisingly, no electronic effect of the ligands on the selectivity for linear aldehyde is observed.[42] The selectivities for linear aldehyde are all between 92 and 93%. The l:b ratio and the isomerization to 2-octene, however, both increase with decreasing phosphine basicity. The increase in l:b ratio with decreasing phosphine basicity can be attributed completely to an increased tendency of the branched alkyl rhodium species to form 2-octene instead of branched aldehyde (Scheme 3). The increasing electrophilicity of the rhodium center leads to a higher reactivity of the rhodium alkyl species toward CO dissociation and β-hydrogen elimination.[26] The total amount of all other products (branched aldehyde and 2-octene) is 7−8% for all ligands.

The constant selectivity for linear aldehyde in the hydroformylation of 1-octene implies that for the basic ligands the l:b ratio reflects the regioselectivity of the formation of the rhodium alkyl species. For the less basic ligands the increase in l:b ratio results from the different behavior of branched and linear rhodium alkyls toward β-hydrogen elimination, as was already reported by Lazaroni and co-workers for the deuterioformylation of 1-hexene.[43] The linear alkyl is mainly converted to linear aldehyde, while the branched alkyl partially generates 2-octene. Since 2-octene is far less reactive in the hydroformylation, its formation is essentially irreversible when 1-octene is still present. We conclude that for our catalytic system the ratio of linear to branched rhodium alkyl species formed is determined not by phosphine basicity but by steric constraints only. Since the natural bite angles for all ligands are virtually the same, this steric parameter seems to explain best the observed constant selectivity for linear aldehyde in this series of ligands.

Hydroformylation of Styrene. The hydroformylation of styrene was carried out at 120 °C and 10 bar of CO/H_2 (1:1) using a 0.50 mM solution of rhodium diphosphine catalyst prepared from $Rh(CO)_2$(dpm) and 10 equiv of ligand. Styrene is a substrate having a distinct preference for the formation of the branched aldehyde due to the stability of the benzylic rhodium species, induced by the formation of a stable η^3 complex.[3] The formation of the linear aldehyde can be enhanced by using high temperature and low pressure.[10,44] The production of 1-phenylpropionaldehyde and 2-phenylpropionaldehyde was monitored by gas chromatography. The results of the experiments with the ligands **1**−**7** are shown in Table 8. Turnover frequencies were determined at 20% conversion.

In the hydroformylation of styrene a regular increase in rate with decreasing phosphine basicity is observed. The increase in activity is accompanied with an increase in l:b ratio and selectivity for linear aldehyde. Although this may seem paradoxical at first, this is not in disagreement with the results obtained in the hydroformylation of 1-octene. Of course styrene behaves rather different in the hydroformylation compared to 1-octene due to the formation of a stable η^3 complex. The reactions were not performed under identical conditions, but the results obtained with both substrates can still be explained similarly. As found for 1-octene the increase in l:b ratio with decreasing phosphine basicity is probably caused by enhanced β-hydrogen elimination. However, for styrene, this does not result in isomerization since β-hydrogen elimination will always result in reformation of styrene. The only effect of enhanced β-hydrogen elimination is an increase in l:b ratio and selectivity for linear aldehyde, as was already explained by Lazaroni and co-workers for the deuterioformylation of styrene.[44,45]

Table 8. Results of the Hydroformylation of Styrene at 120 °C[a]

ligand	R	σ_p	l:b ratio[b]	% select[b]	tof[b,c]
1	$N(CH_3)_2$	−0.83	0.75	43	1100
2	OCH_3	−0.27	0.85	46	1800
3	CH_3	−0.17	1.1	53	2800
4	H	0.00	1.3	56	3100
5	F	0.06	1.3	56	2900
6	Cl	0.23	1.4	59	3200
7	CF_3	0.54	1.8	64	3400

[a] Conditions: $CO/H_2 = 1$, $P(CO/H_2) = 10$ bar, ligand/Rh = 10, substrate/Rh = 1746, [Rh] = 0.50 mM, number of experiments = 3. In none of the experiments was hydrogenation observed. [b] Linear over branched ratio, percent selectivity for linear aldehyde, and turnover frequency were determined at 20% alkene conversion. [c] Turnover frequency = (mol of aldehyde) (mol of Rh)$^{-1}$ h^{-1}.

Discussion

Our results are in contradiction with the earlier studies of Moser and co-workers and Unruh and Christenson.[25,26] This can be explained by the fact that in their ligand systems a strict separation of steric and electronic effects may not have been obtained. In the series of substituted thixantphos ligands steric differences are minimal and only electronic effects are displayed. In the present study we find that there is no influence of phosphine basicity on linear aldehyde selectivity.

Casey and co-workers correlated the regioselectivity of the hydroformylation both with the natural bite angle and the chelation mode of diphosphines in the five-coordinate hydride complexes.[17,18] No plausible explanation, however, has yet been found for the observed trends.[27] From our results it can be concluded that the coordination mode in the five-coordinated hydrido complexes by itself is not crucial in the determination of the regioselectivity of the reaction. Regioselectivity cannot be correlated with the (predominant) chelation mode of the ligands **1**−**7** in the (diphosphine)$Rh(CO)_2H$ complexes, since the ratio of **ee** and **ea** isomers varies from almost 1 for ligand **1** to more than 9 for ligand **7**, while the selectivity for linear aldehyde remains the same for all ligands. Instead, the natural bite angle (obtained from MM2) seems to display a higher correlation with the regioselectivity! Naturally, the observed structures of the (diphosphine)$Rh(CO)_2H$ complexes need not be identical to the structures of the (diphosphine)Rh(CO)H(alkene) complexes, which escape direct observation.

(42) Selectivity for linear aldehyde is the percentage of 1-nonanal of all products including 2-octene.

(43) Lazzaroni, R.; Uccello-Barretta, G.; Benetti, M. *Organometallics* **1989**, *8*, 2323−2327.

(44) Lazzaroni, R.; Raffaelli, A.; Settambolo, R.; Bertozzi, S.; Vitulli, G. *J. Mol. Catal.* **1989**, *50*, 1−9.

(45) Lazzaroni, R.; Settambolo, R.; Raffaelli, A.; Pucci, S.; Vitulli, G. *J. Organomet. Chem.* **1988**, *339*, 357−365.

Scheme 4

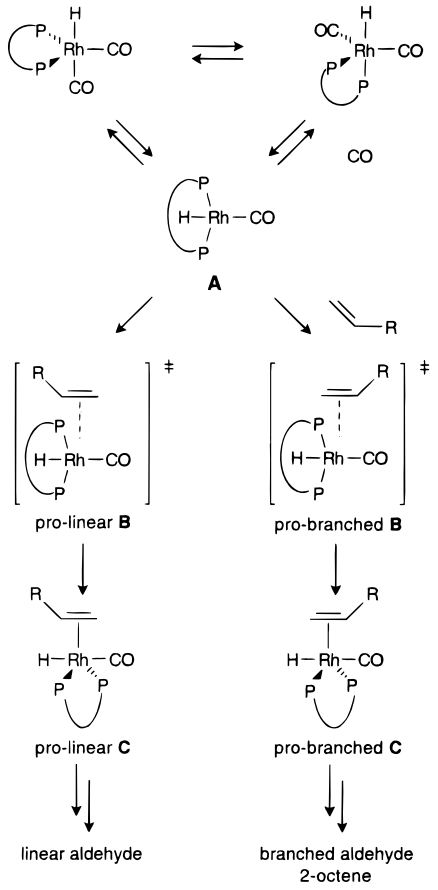

The fact that in our system the **ee**:**ea** isomer ratio does not influence regioselectivity suggests that CO dissociation from both isomeric (diphosphine)$Rh(CO)_2H$ complexes gives the same reactive four-coordinate (diphosphine)Rh(CO)H intermediate (**A**) in the hydroformylation cycle (Scheme 4). In this context it is important to note that the isomerization reaction of **ee** and **ea** isomers is very fast. We were unable to freeze the fluxional behavior in the NMR spectrum even at 163 K, which indicates that the energy barrier for the interconversion of the two isomers is very low, probably less than 10 kcal mol^{-1}. Following CO dissociation from the (diphosphine)$Rh(CO)_2H$ complexes, the regioselectivity in the hydroformylation will be determined by two consecutive steps of alkene coordination and hydride migration. Here we suggest that the regioselectivity is controlled by the alkene attack on the four-coordinate intermediate **A** via a square-pyramidal transition state **B** (Scheme 4). Increasing the bite angle of the diphosphine in intermediate **A** results in increased embracing of the rhodium center by the ligand and consequently in more steric hindrance for the alkene entering the coordination sphere. The hindrance is different for the pro-linear and pro-branched transition states **B**. The preference for the formation of pro-linear over pro-branched **B** is not only determined by the magnitude of the bite angle in intermediate **A**. Although two PPh_3 ligands will induce a larger P−Rh−P angle in intermediate **A**, selectivities for linear aldehyde are much higher for diphosphines such as thixantphos and BISBI, that will probably give bite angles of only ±150° (vide infra). Inspection of the molecular models shows that the backbone of the diphosphine plays a key role in the determination of the relative stabilities of linear and branched isomers of complex **C**. The backbone constrains the orientation of the phenyl substituents of the diphosphines in such a way that formation of linear **C** is favored over that of branched **C**. Modeling studies are currently in progress to substantiate this further.

The existence of a transient four-coordinate $L_2Rh(CO)H$ species in the hydroformylation was already postulated by Wilkinson and co-workers.[7,16,46] Yoshida and co-workers have shown that coordinatively unsaturated trans $L_2Rh(CO)H$ complexes can be stabilized and isolated by the use of sterically bulky phosphine ligands (L = PCy_3 or P-*i*-Pr_3).[47] The X-ray crystal structure of $(PCy_3)_2Rh(CO)H$ was later reported by Freeman and Young.[48] The crystal structure has a square-planar complex geometry with the two phosphines in a trans relation and a P−Rh−P angle of 164.1°. Morokuma and co-workers have calculated the potential and free energy profile of the full cycle of ethylene hydroformylation catalyzed by the $(PH_3)_2Rh(CO)H$ complex using ab initio molecular orbital theory.[37,49] The optimized structure of the intermediate $(PH_3)Rh(CO)_2H$ complex was found to be square planar, and the structures of the transition states between the $(PH_3)Rh(CO)_2H$ and $(PH_3)Rh(CO)_2H(C_2H_4)$ complex were found to be square pyramidal. Herrmann and co-workers have recently calculated the equilibrium structures of both the square-planar four-coordinate $(PH_3)Rh(CO)_2H$ and $(PH_3)_2Rh(CO)H$ complex using DFT theory.[32] The ideal geometry of the $(PH_3)_2Rh(CO)H$ complex was found to have the phosphine groups positioned in a trans relationship and bent toward the hydride.

Evidence for the assumption that even a thixantphos ligand with calculated flexibility range for rhodium of 92−124° can accommodate a trans square-planar geometry can be found in the crystal structure of the (*p*-$(CH_3)_2$N-thixantphos)$Ni(CN)_2$ complex.[50,51] In this distorted square-planar d^8 complex *p*-$(CH_3)_2$N-thixantphos spans two trans positions with a P−Ni−P angle of 151.5°. In the proposed transition states **B** (Scheme 4), the thixantphos or BISBI ligands also span trans positions with P−Rh−P angles around 150−160° and the phosphorus atoms are bent toward the hydride. This complex geometry induced by the ligand backbone and the bite angle controls the orientation of the substituents on the phosphorus atoms, which on their turn determine the relative stabilities of the transition states **B** and/or of the isomers **C**.

The assumption that four-coordinate (diphosphine)Rh(CO)H complexes play a key role in the hydroformylation not only explains the effect of the bite angle on the regioselectivity but also explains the effect on the activity of the reaction. The natural bite angle influences the relative stabilities of the transient four-coordinate complexes and thus the activity of these intermediates. A diphosphine with a natural bite angle close to 90° cannot form a trans square-planar complex but will give an energetically less favorable cis complex.[32] A diphosphine that can accommodate bite angles up to 160°, such as BISBI,[17] can lead to the formation of a trans square-planar complex of lower relative energy (two monodentate phosphines will of course give the most stable trans complex due to the lack of bite angle constraints). A higher stability of the transient four-coordinate (diphosphine)Rh(CO)H intermediate can result in a

(46) Yagupsky, G.; Brown, C. K.; Wilkinson, G. *J. Chem. Soc. A* **1970**, 1392−1401.
(47) Yoshida, T.; Okano, T.; Ueda, Y.; Otsuka, S. *J. Am. Chem. Soc.* **1981**, *103*, 3411−3422.
(48) Freeman, M. A.; Young, D. A. *Inorg. Chem.* **1986**, *25*, 1556−1560.
(49) Koga, N.; Jin, S. Q.; Morokuma, K. *J. Am. Chem. Soc.* **1988**, *110*, 3417−3425.
(50) Goertz, W. Ph.D. Thesis, Rheinisch-Westfälischen Technischen Hochschule Aachen, 1998.
(51) Goertz, W.; Keim, W.; Vogt, D.; Englert, U.; Boele, M. D. K.; van der Veen, L. A.; Kamer, P. C. J.; van Leeuwen, P. W. N. M. *J. Chem. Soc., Dalton Trans.* **1998**, 2981−2988.

higher concentration of the intermediate and/or in a lower activation energy for its formation. If the decrease in activation energy for CO dissociation is accompanied by only a small increase in activation energy for alkene coordination to the four-coordinate complex, then both the higher reactant concentration and the lower activation energy can explain the observed increase in hydroformylation activity with increasing natural bite angle.[10,17]

Conclusion

A pronounced effect of phosphine basicity on the chelation mode of the ligands in the (diphosphine)$Rh(CO)_2H$ complexes was observed. The **ee**:**ea** isomer ratio, observed in the IR and ^1H NMR spectra, showed a regular increase with decreasing phosphine basicity. The spectroscopic results were supported by theoretical calculations using DFT. The electronic ligand effect on catalysis is reflected in both hydroformylation rate and rate of β-hydrogen elimination. Most remarkably, in the hydroformylation of 1-octene, the overall selectivity for linear aldehyde is not influenced by phosphine basicity. Apparently, the chelation mode in the (diphosphine)$Rh(CO)_2H$ complexes per se does not determine the regiochemistry in the hydroformylation reaction and the selectivity for linear aldehyde formation correlates better to the calculated natural bite angle.

Up to now the role of the four-coordinate $L_2Rh(CO)H$ complexes in the hydroformylation has been underestimated. In finding explanations for ligand effects on catalytic performance, attention is focused mainly on the step that converts the more stable five-coordinate $L_2Rh(CO)H$(alkene) complexes into four-coordinate $L_2Rh(CO)$(alkyl) complexes. However, as stated by Casey and co-workers, "*The regioselectivity of hydroformylation is governed by a complex web of electronic and steric effects that have so far defied unraveling.*" [27] Our results clearly indicate that an explanation for the effect of the bite angle on the regioselectivity and activity in the rhodium diphosphine catalyzed hydroformylation is not found in the structure of the five-coordinate (diphosphine)$Rh(CO)_2H$ complexes. The role of the four-coordinate (diphosphine)Rh(CO)H complexes in the reaction can lead to an alternative plausible explanation of the bite angle effect.

Experimental Section

Computational Details. a. DFT Calculations. All DFT calculations were performed with the Amsterdam Density Functional (ADF) program.[52−54] The valence molecular orbitals were expanded in a large basis set of Slater's type orbitals (STOs), whereas the frozen core approximation was used to treat the core electrons. The frozen core orbitals have been taken from atomic calculations in a very large basis set, and quasirelativistic corrections using the Pauli formalism were applied to obtain the frozen core shells. For rhodium, the atomic orbitals up to 3d shell were kept frozen and a triple-ζ basis set with one p polarization function was used. For phosphorus, carbon, oxygen, and fluor, the triple-ζ basis set with one d polarization function was selected, keeping the 2p for phosphorus and the 1s for C, O, and F frozen. The basis set used for hydrogen was also a triple-ζ with one p function for polarization. For the energy calculations the local exchange-correlation potential (LDA) parametrized by Vosko, Wilk, and Nusair[55] was used, in combination with the gradient-corrected (GGA) Becke's[56] functional for exchange and Perdew's[57] functional for correlation (BP86). The GGA approach was applied self-consistently in energy calculations as well as in the geometry optimizations.[58] Geometries were fully optimized under the constrains of the C_s or C_{3v} symmetry group. Second derivatives were evaluated numerically with a two point formula.

b. MM2 Calculations. The molecular mechanics calculations were performed using the CAChe WorkSystem version 3.9,[59] on an Apple Power Macintosh 950, equipped with two CAChe CXP coprocessors. Calculations were carried out similarly to the method described by Casey and Whiteker,[23] using a Rh−P bond length of 2.315 Å. Minimization's were done via the block-diagonal Newton−Raphson method, allowing the structures to converge fully with a termination criterion of a rms factor of 0.0001 kcal $mol^{-1}Å^{-1}$ or less.

General Procedure. All reactions were carried out using standard Schlenk techniques under an atmosphere of purified argon or nitrogen. Toluene and TMEDA were distilled from sodium, THF and diethyl ether from sodium/benzophenone, and hexanes from sodium/benzophenone/triglym. Methanol, ethanol, 1-propanol, and dichloromethane were distilled from CaH_2. Chemicals were purchased from Acros Chimica and Aldrich Chemical Co. $(PPh_3)_3Rh(CO)H$,[60] $Rh(CO)_2$(dpm),[61] and 2,7-dimethylphenoxathiin[62] were prepared according to literature procedures. Silica gel 60 (230−400 mesh) purchased from Merck was used for column chromatography. Melting points were determined on a Gallenkamp MFB-595 melting point apparatus in open capillaries and are uncorrected. NMR spectra were obtained on a Bruker AMX 300 or a DRX 300 spectrometer. ^{31}P and ^{13}C spectra were measured ^1H decoupled. TMS was used as a standard for ^1H and ^{13}C NMR and H_3PO_4 for ^{31}P NMR. Mass spectroscopy was measured on a JEOL JMS-SX/SX102A. Elemental analyses were carried out on an Elementar Vario EL apparatus. Infrared spectra were recorded on a Nicolet 510 FT-IR spectrophotometer. HP-IR spectra were measured using a 20-mL homemade stainless steel autoclave equipped with mechanical stirring and ZnS windows. Hydroformylation reactions were carried out in a 200-mL homemade stainless steel autoclave. Syn gas (CO/H_2, 1:1, 99.9%) and CO (99.9%) were purchased from Air Liquide. D_2 was purchased from Hoekloos. Gas chromatographic analyses were run on an Interscience HR GC Mega 2 apparatus (split/splitless injector, J&W Scientific, DB1 30-m column, film thickness 3.0 mm, carrier gas 70 kPa He, FID detector) equipped with a Hewlett-Packard Data system (Chrom-Card).

4,5-Bis(dichlorophosphino)-2,7-dimethylphenoxathiin (8).[30] At 0 °C, 55.0 mL of *n*-butyllithium (2.5 M in hexanes, 137 mmol) was added dropwise to a stirred mixture of 12.5 g of 2,7-dimethylphenoxathiin (54.8 mmol) and 21.0 mL of TMEDA (137 mmol) in 250 mL of diethyl ether. The reaction mixture was slowly warmed to room temperature and stirred for 16 h. Then the dark yellow solution was cooled to 0 °C, and 74.0 mL of zinc chloride (1.85 M in diethyl ether, 137 mmol) was added dropwise. The reaction mixture decolorized, and a white precipitate was formed. After being stirred for 2 h at room temperature, the reaction mixture was cooled to −196 °C using liquid nitrogen. Then 275 mL of phosphorus chloride (3.2 mol) was distilled onto the frozen reaction mixture. The reaction mixture was warmed to −110 °C, and mechanical stirring was started as soon as possible. The temperature was allowed to rise slowly, and at −50 °C, the colorless reaction mixture became yellow. At room temperature, the reaction mixture was evaporated in vacuo and the resulting residue was extracted with diethyl ether. The solvent was removed in vacuo, and the obtained product was crystallized from hexanes. Yield: 14.3 g of light yellow crystals (61%). Mp: 124−126 °C. ^1H NMR ($CDCl_3$): $\delta = 7.60$ (bs, 2H, $H^{1,8}$), 7.08 (bs, 2H, $H^{3,6}$), 2.36 (s, 6H, CH_3). $^{31}P\{^1H\}$ NMR ($CDCl_3$): $\delta =$ 155.4. $^{13}C\{^1H\}$ NMR (C_6D_6): $\delta = 149.7$ (t, J(P,C) = 28.8 Hz, OC),

(52) Guerra, C. F.; Visser, O.; Snijders, J. G.; te Velde, G.; Baerends, E. J. In *Methods and Techniques in Computational Chemistry, METECC-95*; Clementi, E., Corongiu, G., Eds.; Cagliari: Stef, 1995; p 307.
Baerends, E. J.; Ros, P. *Chem. Phys.* **1973**, *2*, 41.
(54) te Velde, G.; Baerends, E. J. *J. Comput. Phys.* **1992**, *99*, 84.
(55) Vosko, S. H.; Wilk, L.; Nusair, M. *Can. J. Phys.* **1980**, *58*, 1200.
(56) Becke, A. D. *Phys. Rev. A* **1988**, *38*, 3098.
(57) Perdew, J. P. *Phys. Rev. B* **1986**, *33*, 8822−8824.
(58) Fan, L.; Versluis, L.; Ziegler, T.; Baerends, E. J.; Ravenek, W. *Int. J. Quantum Chem., Quantum Chem. Symp.* **1988**, *S22*, 173.
(59) CAChe Scientific Inc., 18700 N.W. Walker Road, Building 92-01, Beaverton, OR 97006.
(60) Ahmad, N.; Levison, J. J.; Robinson, S. D.; Uttley, M. F. *Inorg. Synth.* **1974**, *15*, 59−60.
(61) Coolen, H. K. A. C.; van Leeuwen, P. W. N. M.; Nolte, R. J. M. *J. Org. Chem.* **1996**, *61*, 4739−4747.
(62) Suter, C. M.; McKenzie, J. P.; Maxwell, C. E. *J. Am. Chem. Soc.* **1936**, *58*, 717−720.

135.43, 130.9, 129.0, 128.6 (t, J(P,C) = 64.9 Hz, $C^{4,5}$), 119.5. IR (KBr, cm^{-1}): 2923 (w), 2416 (w), 1436 (m), 1428 (m), 1141 (s), 1104 (s), 987 (s).

Thixantphos Ligands 1−7. In a typical experiment, a solution of 3.52 g of 4-bromo-*N*,*N*-dimethylaniline (17.6 mmol) in 20 mL of THF was added dropwise to a stirred mixture of 0.64 g of magnesium turnings (26.4 mmol), activated with 0.05 mL of 1,2-dibromoethane (0.6 mmol), in 5 mL of THF at room temperature. The reaction mixture was stirred for three h. The reaction mixture was filtered and added to a stirred solution of 1.50 g of **8** (3.52 mmol) in 15 mL of THF at 0 °C. The reaction mixture was slowly warmed to room temperature and stirred for another 3 h. The beige reaction mixture was hydrolyzed with 5 mL of water, and the solvent was removed in vacuo. The resulting brown residue was dissolved in CH_2Cl_2 and washed with dilute HCl. The organic layer was separated, and the aqueous layer was extracted CH_2Cl_2. The combined organic layers were dried with $MgSO_4$, and the solvent removed in vacuo. The resulting white powder was washed with hexanes and recrystallized from toluene. Yield: 1.43 g of pure *p*-$(CH_3)_2$N-thixantphos (**1**) as a white microcrystalline powder (53%). All thixantphos ligands **1**−**7** were fully characterized. Detailed descriptions of the syntheses and characterizations are included in the Supporting Information.

(*p*-$(CH_3)_2$N-Thixantphos)Rh(CO)H(PPh_3) (9a). A solution of $(PPh_3)_3$Rh(CO)H (92 mg, 0.10 mmol) and **1** (85 mg, 0.11 mmol) in 3 mL of toluene was stirred for 0.5 h at 70 °C. The solvent was removed in vacuo ,and the resulting yellow solid was washed with ethanol. ^{1}H NMR (C_6D_6): δ = 7.77 (m, 10H, PPh_3), 7.50 (m, 4H, PPh_3), 7.12 (m, 1H, PPh_3), 6.99 (m, 10H, PCCH, $H^{1,8}$), 6.81 (bs, 2H, $H^{3,6}$), 6.29 (d, ^3J(H,H) = 8.6 Hz, 4H, $(CH_3)_2$NCC*H*), 6.24 (d, ^3J(H,H) = 8.7 Hz, 4H, $(CH_3)_2$NCC*H*), 2.51 (s, 12H, $(CH_3)_2$N), 2.43 (s, 12H, $(CH_3)_2$N), 1.78 (s, 6H, CH_3), −9.09 (dt, ^2J(P,H) = 21 Hz, ^2J(P,H) = 11 Hz, 1H, RhH). ^{31}P{^{1}H} NMR (C_6D_6): δ = 43.4 (dt, ^1J(Rh,P) = 167 Hz, ^2J(P,P) = 125 Hz; PPh_3), 24.7 (dd, ^1J(Rh,P) = 147 Hz, ^2J(P,P) = 125 Hz). IR (KBr, cm^{-1}): 1982 (s, HRhCO), 1909 (m, HRhCO).

(*p*-$(CH_3)_2$N-Thixantphos)Rh$(CO)_2$H (9b). A solution of $Rh(CO)_2$(acac) (13 mg, 50 μmol) and **1** (39 mg, 50 μmol) in 1.0 mL of C_6D_6 was pressurized with 20 bar of CO/H_2 (1:1) and left overnight at 80 °C. ^{1}H HP-NMR (C_6D_6): δ = 7.61 (m, 8H, PCCH), 6.75 (s, 2H, $H^{1,8}$), 6.63 (d, ^2J(P,H) = 6.0 Hz, $H^{3,6}$), 6.22 (d, ^3J(H,H) = 8.1 Hz, $(CH_3)_2$NCC*H*), 2.39 (s, 24H, $(CH_3)_2$N), 1.65 (s, 3H, CH_3), −8.25 (dt, ^1J(Rh,H) = 8.7 Hz, ^2J(P,H) = 27.9 Hz, 1H, RhH). ^{31}P{^{1}H} HP-NMR (C_6D_6): δ = 19.8 (d, ^1J(Rh,P) = 121 Hz). HP-IR (2-MeTHF, cm^{-1}): 2027 (RhCO), 1983 (RhCO), 1960 (RhCO), 1935 (RhCO), 1596 (CO-dpm).

(*p*-CH_3O-Thixantphos)Rh(CO)H(PPh_3) (10a). This compound was prepared similarly to **9a**. Orange yellow crystals suitable for X-ray structure determination were obtained from toluene/ethanol. ^{1}H NMR (C_6D_6): δ = 6.68 (m, 10H, PPh_3), 7.41 (m, 4H, PPh_3), 7.04 (m, 1H, PPh_3), 6.93 (m, 8H, PCCH), 6.80 (d, ^4J(H,H) = 1.6 Hz, 2H, $H^{1,8}$), 6.61 (bs, 2H, $H^{3,6}$), 6.51 (d, ^3J(H,H) = 8.6 Hz, 4H, CH_3OCC*H*), 6.47 (d, ^3J(H,H) = 8.7 Hz, 4H, CH_3OCC*H*), 3.32 (s, 6H, CH_3O), 3.25 (s, 6H, CH_3O), 1.77 (s, 6H, CH_3), −9.33 (dt, ^2J(P,H) = 20 Hz, ^2J(P,H) = 11 Hz, 1H, RhH). ^{31}P{^{1}H} NMR (C_6D_6): δ = 43.4 (dt, ^1J(Rh,P) = 163 Hz, ^2J(P,P) = 124 Hz; PPh_3), 25.7 (dd, ^1J(Rh,P) = 148 Hz, ^2J(P,P) = 124 Hz). IR (KBr, cm^{-1}): 1989 (s, HRhCO), 1916 (m, HRhCO). Anal. Calcd for $C_{61}H_{54}O_6P_3RhS$: C, 65.95; H, 4.90; S, 2.89. Found: C, 66.14; H, 5.03; S, 3.23.

X-ray Crystal Structure Determination of 10a. 10a crystallized in the triclinic space group $P\bar{1}$, a = 10.7820(7) Å, b = 11.707(3) Å, c = 23.322(2) Å, α = 86.737(9)°, β = 78.718(6)°, γ = 68.24(1)°, V = 2682.1(9) Å^3, and Z = 2. The data collection was carried out at room temperature. The structure was solved by direct methods. The hydrogen atoms were calculated. The structure was refined to R = 0.067 and R_w = 0.085, for 9235 observed reflections. Crystal data and collection parameters, atomic coordinates, bond lengths, bond angles, and thermal parameters are included in the Supporting Information.

(*p*-CH_3O-Thixantphos)Rh$(CO)_2$H (10b). This compound was prepared similarly to **9b**. ^{1}H HP-NMR (C_6D_6): δ = 7.46 (bs, 8H, PCCH), 6.73 (s, 2H, $H^{1,8}$), 6.43 (bs, 8H, CH_3OCC*H*), 6.30 (bs, 2H, $H^{3,6}$), 3.20 (s, 12H, CH_3O), 1.64 (s, 6H, CH_3), −8.25 (dt, ^1J(Rh,H) = 7.5 Hz, ^2J(P,H) = 21.6 Hz, 1H, RhH). ^{31}P{^{1}H} HP-NMR (C_6D_6): δ = 21.7 (d, ^1J(Rh,P) = 124 Hz). HP-IR (2-MeTHF, cm^{-1}): 2034 (RhCO), 1990 (RhCO), 1966 (RhCO), 1942 (RhCO), 1595 (CO-dpm).

(*p*-CH_3-Thixantphos)Rh(CO)H(PPh_3) (11a). This compound was prepared similarly to **9a**. Orange crystals were obtained from toluene/ethanol. ^{1}H NMR (C_6D_6): δ = 7.73 (m, 10H, PPh_3), 7.46 (bm, 4H, PPh_3), 7.21 (s, 2H, $H^{1,8}$), 7.08 (m, 1H, PPh_3), 6.98 (m, 8H, PCCH), 6.81 (d, ^3J(H,H) = 8.2 Hz, 4H, CH_3CC*H*), 6.75 (d, ^3J(H,H) = 7.9 Hz, 4H, CH_3CC*H*), 6.69 (s, 2H, $H^{3,6}$), 2.12 (s, 12H, CH_3 tolyl), 2.04 (s, 12H, CH_3 tolyl), 1.78 (s, 6H, CH_3), −9.23 (dt, ^2J(P,H) = 20 Hz, ^2J(P,H) = 12 Hz, RhH). ^{31}P{^{1}H} NMR (C_6D_6): δ = 43.6 (dt, ^1J(Rh,P) = 167 Hz, ^2J(P,P) = 123 Hz; PPh_3), 26.8 (dd, ^1J(Rh,P) = 148 Hz, ^2J(P,P) = 124 Hz). IR (KBr, cm^{-1}): 1999 (s, HRhCO), 1920 (m, HRhCO).

(*p*-CH_3-Thixantphos)Rh$(CO)_2$H (11b). This compound was prepared similarly to **9b**. ^{1}H HP-NMR (C_6D_6): δ = 7.51 (bs, 8H, PCCH), 6.68 (d, ^3J(H,H) = 8.1 Hz, CH_3CC*H*), 6.56 (bs, 2H, $H^{1,8}$), 6.42 (d, ^2J(P,H) = 5.1 Hz, $H^{3,6}$), 1.93 (s, 12H, CH_3 tolyl), 1.60 (s, 6H, CH_3), −8.52 (dt, ^1J(Rh,H) = 7.2 Hz, ^2J(P,H) = 17.6 Hz, 1H, RhH). ^{31}P-{^{1}H} HP-NMR (C_6D_6): δ = 22.7 (d, ^1J(Rh,P) = 126 Hz). HP-IR (2-MeTHF, cm^{-1}): 2035 (RhCO), 1992 (RhCO), 1969 (RhCO), 1943 (RhCO), 1595 (CO-dpm).

(Thixantphos)Rh(CO)H(PPh_3) (12a). This compound was prepared similarly to **9a** and was already described by Kranenburg and co-workers.[10] Orange yellow crystals suitable for X-ray structure determination were obtained from toluene/ethanol.

X-ray Crystal Structure Determination of 12a. 12a crystallized in the triclinic space group $P\bar{1}$, a = 10.9776(6) Å, b = 11.0845(9) Å, c = 11.730(3) Å, α = 113.77(1)°, β = 94.81(1)°, γ = 108.435(5)°, V = 1201.3(4) Å^3, and Z = 1. The data collection was carried out at room temperature. The structure was solved by direct methods. The hydrogen atoms were calculated. The structure was refined to R = 0.030 and R_w = 0.038, for 4931 observed reflections. Crystal data and collection parameters, atomic coordinates, bond lengths, bond angles, and thermal parameters are included in the Supporting Information.

(Thixantphos)Rh$(CO)_2$H (12b). This compound was prepared similarly to **9b** and was already described by Kranenburg and co-workers.[10]

(Thixantphos)Rh$(CO)_2$D (12-Db). This compound was prepared in situ from **12b** and D_2. HP-IR (2-MeTHF, cm^{-1}): 2019 (RhCO), 1994 (RhCO), 1958 (RhCO), 1947 (RhCO), 1587 (CO-dpm).

(*p*-F-Thixantphos)Rh(CO)H(PPh_3) (13a). This compound was prepared similarly to **9a**. ^{1}H NMR (C_6D_6): δ = 7.54 (m, 10H, PPh_3), 7.28 (m, 4H, PPh_3), 7.09 (m, 1H, PPh_3), 6.96 (m, 8H, PCCH), 6.82 (bs, 2H, $H^{1,8}$), 6.61 (m, 8H, FCCH), 6.40 (bs, 2H, $H^{3,6}$), −9.49 (dt, ^2J(P,H) = 18 Hz, ^2J(P,H) = 11 Hz, 1H, RhH). ^{31}P{^{1}H} NMR (C_6D_6): δ = 42.7 (dt, ^1J(Rh,P) = 167 Hz, ^2J(P,P) = 124 Hz, PPh_3), 26.5 (dd, ^1J(Rh,P) = 149 Hz, ^2J(P,P) = 124 Hz). IR (KBr, cm^{-1}): 2002 (s, HRhCO), 1921 (m, HRhCO). Anal. Calcd for $C_{57}H_{42}F_4O_2P_3RhS$: C, 64.41; H, 3.99; S, 3.02. Found: C, 64.88; H, 4.28; S, 2.68.

(*p*-F-Thixantphos)Rh$(CO)_2$H (13b). This compound was prepared similarly to **9b**. ^{1}H HP-NMR (C_6D_6): δ = 7.19 (bs, 8H, PCCH), 6.70−6.36 (ar), 1.58 (s, 6H, CH_3), −8.97 (dt, ^1J(Rh,H) = 6.3 Hz, ^2J(P,H) = 11.0 Hz, 1H, RhH). ^{31}P{^{1}H} HP-NMR (C_6D_6): δ = 23.3 (d, ^1J(Rh,P) = 130 Hz). HP-IR (2-MeTHF, cm^{-1}): 2041 (RhCO), 1997 (RhCO), 1975 (RhCO), 1950 (RhCO), 1588 (CO-dpm).

(*p*-Cl-Thixantphos)Rh(CO)H(PPh_3) (14a). This compound was prepared similarly to **9a**. ^{1}H NMR (C_6D_6): δ = 7.47 (dd, ^3J(H,H) = 11 Hz, ^3J(H,H) = 8.3 Hz, 6H, PPh_3), 7.36 (m, 4H, PPh_3), 7.17 (bs, 4H, PPh_3), 7.02 (m, 1H, PPh_3), 6.87 (m, 16H), 6.74 (d, ^4J(H,H) = 1.2 Hz, 2H, $H^{1,8}$), 6.36 (bs, 2H, $H^{3,6}$), 1.69 (s, 6H, CH_3), −9.60 (q, ^2J(P,H) = 14 Hz, 1H, RhH). ^{31}P{^{1}H} NMR (C_6D_6): δ = 42.8 (dt, ^1J(Rh,P) = 165 Hz, ^2J(P,P) = 123 Hz; PPh_3), 26.6 (dd, ^1J(Rh,P) = 149 Hz, ^2J(P,P) = 123 Hz). IR (KBr, cm^{-1}): 2006 (s, HRhCO), 1928 (m, HRhCO). Anal. Calcd for $C_{57}H_{42}Cl_4O_2P_3RhS$: C, 60.66; H, 3.75; S, 2.84. Found: C, 61.14; H, 4.13; S, 2.78.

(*p*-Cl-Thixantphos)Rh$(CO)_2$H (14b). This compound was prepared similarly to **9b**. ^{1}H HP-NMR (C_6D_6): δ = 7.25−6.95 (ar), 6.83−6.68 (ar), 1.59 (s, 6H, CH_3), −9.04 (dt, ^1J(Rh,H) = 6.0 Hz, ^2J(P,H) = 8.4 Hz, 1H, RhH). ^{31}P{^{1}H} HP-NMR (C_6D_6): δ = 23.7 (d, ^1J(Rh,P) = 132 Hz). HP-IR (2-MeTHF, cm^{-1}): 2042 (RhCO), 1999 (RhCO), 1977 (RhCO), 1952 (RhCO), 1574 (CO-dpm).

(*p*-CF_3-Thixantphos)Rh(CO)H(PPh_3) (15a). This compound was prepared similarly to **9a**. Orange crystals were obtained from toluene/ethanol. ^{1}H NMR (C_6D_6): δ = 7.43 (m, 10H, PPh_3), 7.19 (m, 4H, PPh_3), 7.02 (t, J = 7.2 Hz, 8H, PCCH), 6.94 (m, 1H, PPh_3), 6.85 (m, 8H, CF_3CCH), 6.75 (d, ^4J(H,H) = 1.6 Hz, 2H, $H^{1,8}$), 6.22 (bs, 2H, $H^{3,6}$), 1.66 (s, 6H, CH_3), −9.43 (q, ^2J(P,H) = 14 Hz, 1H, RhH). ^{31}P-{^{1}H} NMR (C_6D_6): δ = 41.8 (dt, ^1J(Rh,P) = 164 Hz, ^2J(P,P) = 122 Hz, PPh_3), 27.8 (dd, ^1J(Rh,P) = 149 Hz, ^2J(P,P) = 122 Hz). IR (KBr, cm-1): 2009 (s, HRhCO), 1931 (m, HRhCO). Anal. Calcd for $C_{61}H_{42}F_{12}O_2P_3RhS$: C, 58.02; H, 3.35; S, 2.54. Found: C, 57.92; H, 3.47; S, 2.78.

(*p*-CF_3-Thixantphos)$Rh(CO)_2$H (15b). This compound was prepared similarly to **9b**. ^{1}H HP-NMR (C_6D_6): δ = 7.23 (bs, 8H, PCCH), 7.00 (d, ^3J(H,H) = 8.1 Hz, 8H, CF_3CCH), 6.85 (d, ^2J(P,H) = 6.0 Hz, 2H, $H^{3,6}$), 6.71 (s, 2H, $H^{1,8}$), 1.59 (s, 6H, CH_3), −9.07 (dt, ^1J(Rh,H) = 4.5 Hz, ^2J(P,H) = 3.6 Hz, 1H, RhH). ^{31}P{^{1}H} HP-NMR (C_6D_6): δ = 24.7 (d, ^1J(Rh,P) = 134 Hz). HP-IR (2-MeTHF, cm^{-1}): 2046 (RhCO), 2004 (RhCO), 1982 (RhCO), 1957 (RhCO), 1607 (CO-dpm).

Hydroformylation Experiments. Hydroformylation reactions were carried out in an autoclave, equipped with glass inner beaker, a substrate inlet vessel, a liquid sampling valve, and a magnetic stirring rod. The temperature was controlled by an electronic heating mantle. In a typical experiment, the desired amount of ligand was placed in the autoclave and the system was evacuated and heated to 50 °C. After 0.5 h, the autoclave was filled with CO/H_2 (1:1) and a solution of $Rh(CO)_2$(dpm) (5 or 10 μmol) in 8.5 mL of toluene. The autoclave was pressurized to the appropriate pressure (6 or 16 bar), heated to reaction temperature, and stirred for 0.5 h (120 °C) or 1.5 h (80 °C) to form the active catalyst. Then 1.0 mL of substrate (filtered over neutral activated alumina to remove peroxide impurities) and 0.5 mL of the internal standard *n*-decane were placed in the substrate vessel, purged three times with 10 bar CO/H_2 (1:1), and pressed into the autoclave with 10 or 20 bar CO/H_2 (1:1). At the 20% conversion level the reaction was stopped by adding 0.25 mL of tri-*n*-butyl phosphite and cooling on ice. Samples of the reaction mixture were analyzed by temperature-controlled gas chromatography.

HP-FT-IR Experiments. In a typical experiment the HP-IR autoclave was filled with 2−5 equiv of ligand, 5 mg of $Rh(CO)_2$(dpm), and 15 mL of 2-MeTHF. The autoclave was purged three times with 15 bar of CO/H_2 (1:1), pressurized to approximately 18 bar, and heated to 80 °C. Catalyst formation was followed in time by FT-IR and was usually complete within 1 h.[63]

HP-NMR Experiments. In a typical experiment 0.4 mL of a solution of 50 μmol of $Rh(CO)_2$(acac) and 50 μmol of ligand in 1.0 mL of C_6D_6 was transferred into a 0.5-cm sapphire NMR tube. The tube was pressurized with 20 bar of CO/H_2 (1:1) and left overnight at 80 °C. For VT experiments half the amounts of rhodium and ligand were used in 0.5 mL of THF-d_8.

Acknowledgment. Financial support from SON/STW is gratefully acknowledged, and we thank Dr. H. T. Teunissen and Prof. Dr. F. Bickelhaupt for providing the experimental procedure for the synthesis of compound **8**. DFT calculations were carried out on workstations purchased from funds provided by the Spanish Dirección General de Investigación Científica y Técnica (DGICYT) under Project PB95-0639-C02-02 and by the CIRIT of the Generalitat de Catalunya under Project SGR97-17.

Supporting Information Available: Detailed description of the syntheses and characterizations of thixantphos ligands **1**−**7**, HP-IR spectrum of **12-Db** (carbonyl region), and tables of crystal data and collection parameters, atomic coordinates, bond lengths, bond angles, thermal parameters, and H-atom coordinates for **10a** and **12a** (39 pages, print/PDF). See any current masthead page for ordering information and Web access instructions.

JA981969E

(63) Castellanos-Páez, A.; Castillón, S.; Claver, C.; van Leeuwen, P. W. N. M.; de Lange, W. G. J. *Organometallics* **1998**, *17*, 2543−2552.